

An Unstructured Finite-volume Technique for Shallow-water Flows with Wetting and Drying Fronts

Rajendra K. Ray^{1,*}, Kim Dan Nguyen¹

Abstract—An unstructured finite volume numerical model is presented here for simulating shallow-water flows with wetting and drying fronts. The model is based on the Green's theorem in combination with Chorin's projection method. A 2nd-order upwind scheme coupled with a Least Square technique is used to handle convection terms. An Wetting and drying treatment is used in the present model to ensure the total mass conservation. To test its capacity and reliability, the present model is used to solve the Parabolic Bowl problem. We compare our numerical solutions with the corresponding analytical and existing standard numerical results. Excellent agreements are found in all the cases.

Keywords—Finite volume method, Projection method, Shallow water, Unstructured grid, wetting/drying fronts.

I. INTRODUCTION

FREE-surface water flows can be seen in many real life flow situations such as river and lake hydrodynamics, surface irrigation, tides, dam break flows, as well as estuarine and coastal circulation. Many of these flows involve complex flow behaviors, irregular flow domains, rapid variation of bottom topography and moving boundaries in which wetting and drying of variable topography occurs. Satisfactory numerical simulations of these processes are very challenging tasks. Because of these reasons, free-surface flows are gaining popularity amongst the computational fluid dynamics community in the last few decades.

These types of flow behaviors can be modeled mathematically by Shallow-Water Equations (SWE), which are derived by considering the depth-averaged three-dimensional incompressible Navier-Stokes equations, assuming hydrostatic pressure distribution, and neglecting vertical acceleration and viscous effects. The discretization of the SWE has been the subject of extensive literature. Until recent years, the most commonly chosen numerical methods were Finite Differences (FD), Continuous Finite Elements (CFE) and Finite Volumes (FV). The main motivation for using FV is that such methods are especially tailored to discretize conservation laws possibly with shocks, usually producing approximate solutions with local conservation properties.

The unstructured finite-volume methods (UFVMs) not only ensure local mass conservation, but also the best possible fitting of computing meshes into the studied domain

boundaries. Recently, Nguyen *et. al.* [9] has developed an unstructured finite volume methods for computing shallow-water flows in complex topographies and geometries, using the technique based on Green's theorem in combination with Chorin's projection method [4]. In their scheme, Rhie and Chow's technique [10] is introduced for preventing numerical oscillations. The model is validated and approved by several benchmark tests. But, this scheme is unable to conserve the total mass of the physical domain and gives poor results for the moving boundary problems (like dam break flows, Parabolic bowl problem etc.) in which wetting and drying of variable topography occurs.

The purpose of the present work is to extend the above unstructured finite volumes method for moving boundary problems. The same type of idea like Brufau *et. al.* [2], has been used to tackle the drying and flooding situations of the boundary cells of the flow domain. This extended scheme gives very satisfactory results for the moving boundary problems considered here. In the next section, we discuss about the governing equations and projection method. Section 3 discuss about the numerical technique and wetting and drying treatment. In section 4, we validate our scheme by solving the well known test problem of parabolic bowl and finally, section 5 summarizes the whole work.

II. GOVERNING EQUATIONS AND PROJECTION METHOD

A. Governing Equations:

The two-dimensional Shallow-water equations, consist of the depth-averaged continuity equation and x and y momentum equations, can be written as follows:

Continuity equation:

$$\frac{\partial Z_s}{\partial t} + \frac{\partial(hu)}{\partial x} + \frac{\partial(hv)}{\partial y} = 0 \quad (1)$$

Momentum equations:

$$\begin{aligned} & \frac{\partial(hu)}{\partial t} + \frac{\partial(hu^2)}{\partial x} + \frac{\partial(huv)}{\partial y} \\ & = f(hv) - gh \frac{\partial Z_s}{\partial x} + \frac{\partial}{\partial x} \left[A_H \frac{\partial(hu)}{\partial x} \right] + \frac{\partial}{\partial y} \left[A_H \frac{\partial(hu)}{\partial y} \right] - \frac{\tau_{bx}}{\rho_o} \end{aligned} \quad (2)$$

* Correspondence to: Laboratoire d'Hydraulique Saint-Venant, 6 quai Watier, 78400 Chatou, France. E-mail : rajendra.ray@gmail.com

$$\begin{aligned} & \frac{\partial(hv)}{\partial t} + \frac{\partial(huv)}{\partial x} + \frac{\partial(hv^2)}{\partial y} = \\ & -f(hu) - gh \frac{\partial Z_s}{\partial y} + \frac{\partial}{\partial x} \left[A_H \frac{\partial(hv)}{\partial x} \right] + \frac{\partial}{\partial y} \left[A_H \frac{\partial(hv)}{\partial y} \right] - \frac{\tau_{by}}{\rho_0} \end{aligned} \quad (3)$$

where g is the gravity acceleration; f is the Coriolis parameter; u and v are the depth-averaged velocity components in x and y directions respectively; Z_s is the water surface elevation; h is the flow depth and τ_{bx} and τ_{by} are the bed shear stresses determined by Chézy's formula as

$$\frac{\tau_b(x, y)}{\rho_0} = g \frac{\sqrt{u^2 + v^2}}{C_h^2} (u, v) = F(u, v) \quad (4)$$

where C_h is the Chézy coefficient. A_H , the horizontal dispersion coefficient, can be calculated following Elder's formula and applied for 2D flows

$$A_H = 6u_*h,$$

where u_* is the friction velocity that can be defined by

$$u_* = \sqrt{g(x^2 + y^2)} / C_h.$$

B. Projection Method:

Chorin's projection method [4] has been applied here to split up the Saint-Venant equations in the successive steps: convection-diffusion, wave propagation and velocity correction ([6], [8], [9]).

Convection-diffusion step

$$\begin{aligned} \frac{\partial q_x^*}{\partial t} + \frac{\partial(uq_x^*)}{\partial x} + \frac{\partial(vq_x^*)}{\partial y} &= A_H \left[\frac{\partial^2 q_x^*}{\partial x^2} + \frac{\partial^2 q_x^*}{\partial y^2} \right] \\ \frac{\partial q_y^*}{\partial t} + \frac{\partial(uq_y^*)}{\partial x} + \frac{\partial(vq_y^*)}{\partial y} &= A_H \left[\frac{\partial^2 q_y^*}{\partial x^2} + \frac{\partial^2 q_y^*}{\partial y^2} \right] \end{aligned} \quad (5)$$

(5) is transport equations. Subscript (*) is purely symbolic to design values of q_x and q_y , obtained after this step.

Wave propagation step

The combination of the continuity and momentum equations without convection and diffusion terms, allows us to get a Poisson's equation for only water surface levels as unknowns:

$$\left[1 - \frac{\gamma^2 gh}{A} \left(\frac{\partial^2}{\partial x^2} + \frac{\partial^2}{\partial y^2} \right) \right] \delta Z_s = \frac{B}{A}, \quad (6)$$

$$\text{where, } \delta Z_s = Z_s^{n+1} - Z_s^n$$

$$\begin{cases} B = \gamma gh \left(\frac{\partial^2 Z_s^n}{\partial x^2} + \frac{\partial^2 Z_s^n}{\partial y^2} \right) + g \left(\frac{\partial h}{\partial x} \frac{\partial(\delta Z_s)}{\partial x} + \frac{\partial h}{\partial y} \frac{\partial(\delta Z_s)}{\partial y} \right) \\ - \frac{\gamma}{dt} \left(\frac{\partial q_x^*}{\partial x} + \frac{\partial q_y^*}{\partial y} \right) - \gamma \left(\frac{\partial L_x}{\partial x} + \frac{\partial L_y}{\partial y} \right) - \frac{1-\gamma}{dt} \left(\frac{\partial q_x^n}{\partial x} + \frac{\partial q_y^n}{\partial y} \right) \\ A = dt^{-1} (dt^{-1} + \gamma F), \quad F = \frac{g}{C_h^2 h^2} \sqrt{(q_x^n)^2 + (q_y^n)^2}, \\ L_x = \frac{\tau_{wx}}{\rho}, \quad L_y = \frac{\tau_{wy}}{\rho} \end{cases} \quad (7)$$

γ is a time weighting coefficient, $1 \geq \gamma \geq 1/2$. We note that,

the term $g \left(\frac{\partial h}{\partial x} \frac{\partial(\delta Z_s)}{\partial x} + \frac{\partial h}{\partial y} \frac{\partial(\delta Z_s)}{\partial y} \right)$ was ignored in

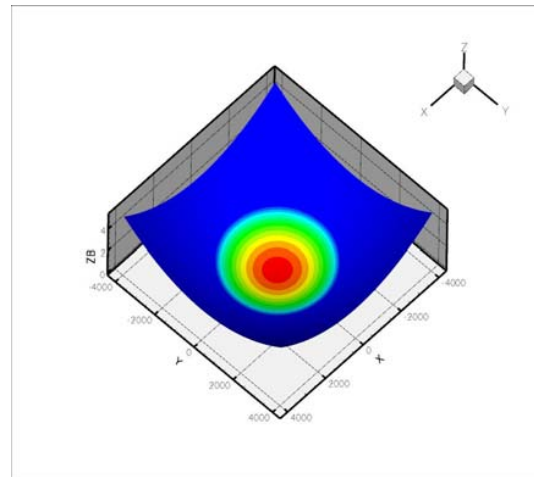
Nguyen et al. [9]. We now introduced it to take into consideration the bottom gradient, which may be large in flows over a very irregular bed.

Velocity correction step

Once the water surface levels are known, the unit discharges q_x^* and q_y^* should be now corrected using the momentum equations:

$$q_x^{n+1} = \left(q_x^* - \gamma gh dt \frac{\partial Z_s^{n+1}}{\partial x} - (1-\gamma) gh dt \frac{\partial Z_s^n}{\partial x} \right) (1 + \gamma F dt)^{-1} (8)$$

$$q_y^{n+1} = \left(q_y^* - \gamma gh dt \frac{\partial Z_s^{n+1}}{\partial y} - (1-\gamma) gh dt \frac{\partial Z_s^n}{\partial y} \right) (1 + \gamma F dt)^{-1} (9)$$



(A)

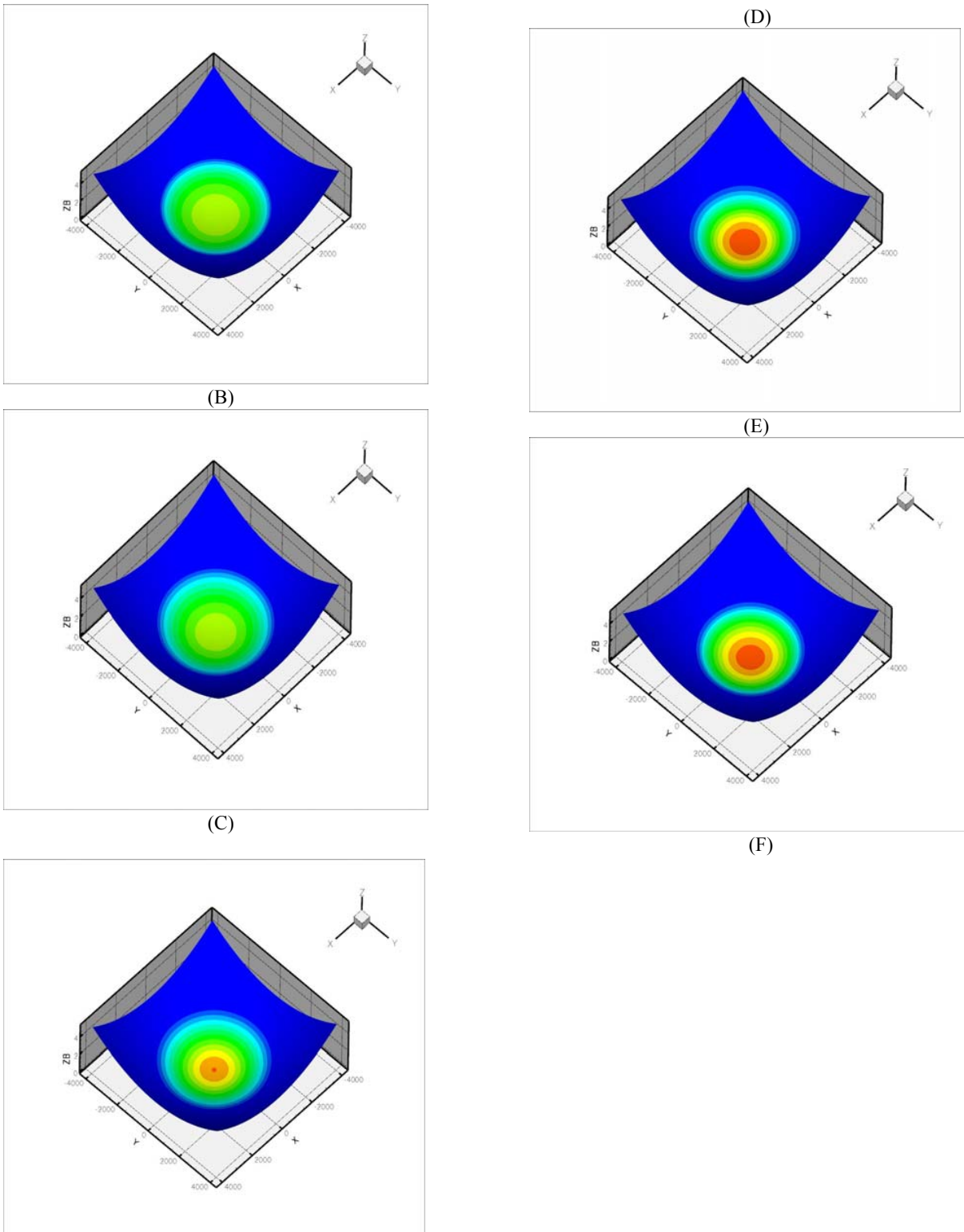


Fig. 1. Parabolic Bowl: Computed water surface elevations at (A) $t = \tau/6$, (B) $t = 2\tau/6$, (C) $t = 3\tau/6$, (D) $t = 4\tau/6$, (E) $t = 5\tau/6$, (F) $t = \tau$.

III. NUMERICAL TECHNIQUES AND WETTING AND DRYING TREATMENT

The present model is based on the Green's theorem in combination with Chorin's projection method [4].

Equations (5)-(9) have been integrated by a technique based on Green's theorem and then discretised by a Unstructured Finite-Volume Method (UFVM). The convection terms are handled by a 2nd order ULSS (Upwind Least Square Scheme, Kobayashi et al. [7]). The linear equation system issued from the wave propagation step is implicitly solved by a SOR (Successive Over Relaxation, Tannehill et al. [11]) technique. The readers can be referred to Nguyen et al [9] for the details of these techniques.

In a fluid flow problem, when wetting front advance over a dry bed or vice versa, the problem is called a moving boundary problem. In the present scheme, to capture the moving boundary and to conserve the total mass of the fluid, we adapt an almost similar treatment like Brufau *et al.* [2]. The main idea in this treatment is to find out the partially drying or flooding cells in each time step and then add or subtract hypothetical fluid mass to fill the cell or to make the cell totally dry respectively, and then subtract or add the same amount of fluid mass to the neighbouring wet cells in the computational domain. To consider a cell to be wet or dry in a given time step, we use the threshold value $\varepsilon = O(10^{-3})$ as the minimum water depth (h). If $h \leq \varepsilon$, the cell will be considered as dry and the water depth for that cell set to be fixed as $h = \varepsilon$ for that time step. The details of this treatment can be found in the paper by Brufau *et al.* [2].

IV. NUMERICAL VALIDATION

Parabolic Bowl:

In this section, we test the capacity of the present model in describing the wetting and drying fronts. The bed topography of the domain is defined by $b(x) = \alpha r^2$, where α is a positive constant and $r^2 = x^2 + y^2$. The analytical solution is periodic in time with a period $\tau = 2\pi/\omega$. The water depth

$h(r, t)$ is non-zero for $r < \sqrt{(X + Y \cos \omega t) / \alpha(X^2 - Y^2)}$

and the analytical solution ([12]) is given within the range as follows:

$$h(r, t) = \frac{1}{X + Y \cos \omega t} + \alpha(Y^2 - X^2) \frac{r^2}{(X + Y \cos \omega t)^2}, \quad (10)$$

$$(u, v)(\vec{x}, t) = -\frac{Y\omega \sin \omega t}{X + Y \cos \omega t} \left(\frac{x}{2}, \frac{y}{2} \right). \quad (11)$$

Here, α , X and Y are fixed as $1.6 \times 10^{-7} m^{-1}$, $1 m^{-1}$ and $-0.41884 m^{-1}$ respectively. The computational domain (Ω) is considered here as a square region $[-4000, 4000] \times [-4000, 4000] m^2$ with an origin at the domain centre. The threshold value ε is set as 3×10^{-3} .

Fig. 1 shows the time evolution of computed solution for six different time stages of a full period (τ). In Figure 2, we plot the 3D water depth (h) for the same time stages. For these computations, we use a (70×70) mesh. Our computed results are matching very well quantitatively, with the corresponding analytical solution of Thacker ([12]) and qualitatively with the existing standard numerical solutions of Bunya *et al.* ([3]) and Ern *et al.* ([5]). The L^2 error norms of the water-depth (h) corresponding to five different mesh sizes, starting from $[13 \times 13]$ to $[200 \times 200]$, at $t = \tau/2$ and $t = \tau$, are shown in Figure 3. It is clear from these figures that in the wetting stage (see Figure 3 [left]) the rate of convergence is more than 1.4 and in the drying stage (see Figure 3 [right]), it is more than 1.3. Both the convergence rates are better than that of Bunya *et al.* ([3]) and Ern *et al.* ([5]). Moreover, it can be noticed that both, Ern *et al.* (2008) and Bunya *et al.* (2009) got convergence rates, which are totally different for wetting and drying stages with convergence rates decreasing in the latter stage, whereas the convergence rates obtained from our scheme remain almost the same for both stages. This certainly proves the efficiency and robustness of the present numerical scheme in treating the wetting-drying-wetting transitions. Figure 4 plots the L^2 error norms at $t = \tau/2$ and $t = \tau$ for different Courant numbers that can reach up to 1.2. This proves the unconditional stability of the present scheme that is fully implicit. Clearly, the L^2 errors are still bounded for the Courant number even greater than 1. In all the computations for different mesh-sizes, the relative error in global mass conservation has been found less than 0.003%, which confirms that our numerical scheme correctly respects the total mass conservation.

V. CONCLUSION

In this paper we extended an unstructured finite volume scheme, developed by Nguyen et al. [9], for the moving boundary problems in which wetting and drying fronts occur. This extended method correctly conserve the total mass of the physical domain. To validate our scheme, we solve the parabolic bowl problem. Our scheme very efficiently capture the wetting-drying-wetting transitions and shows almost 1.4 order of accuracy for both the wetting and drying stages. This

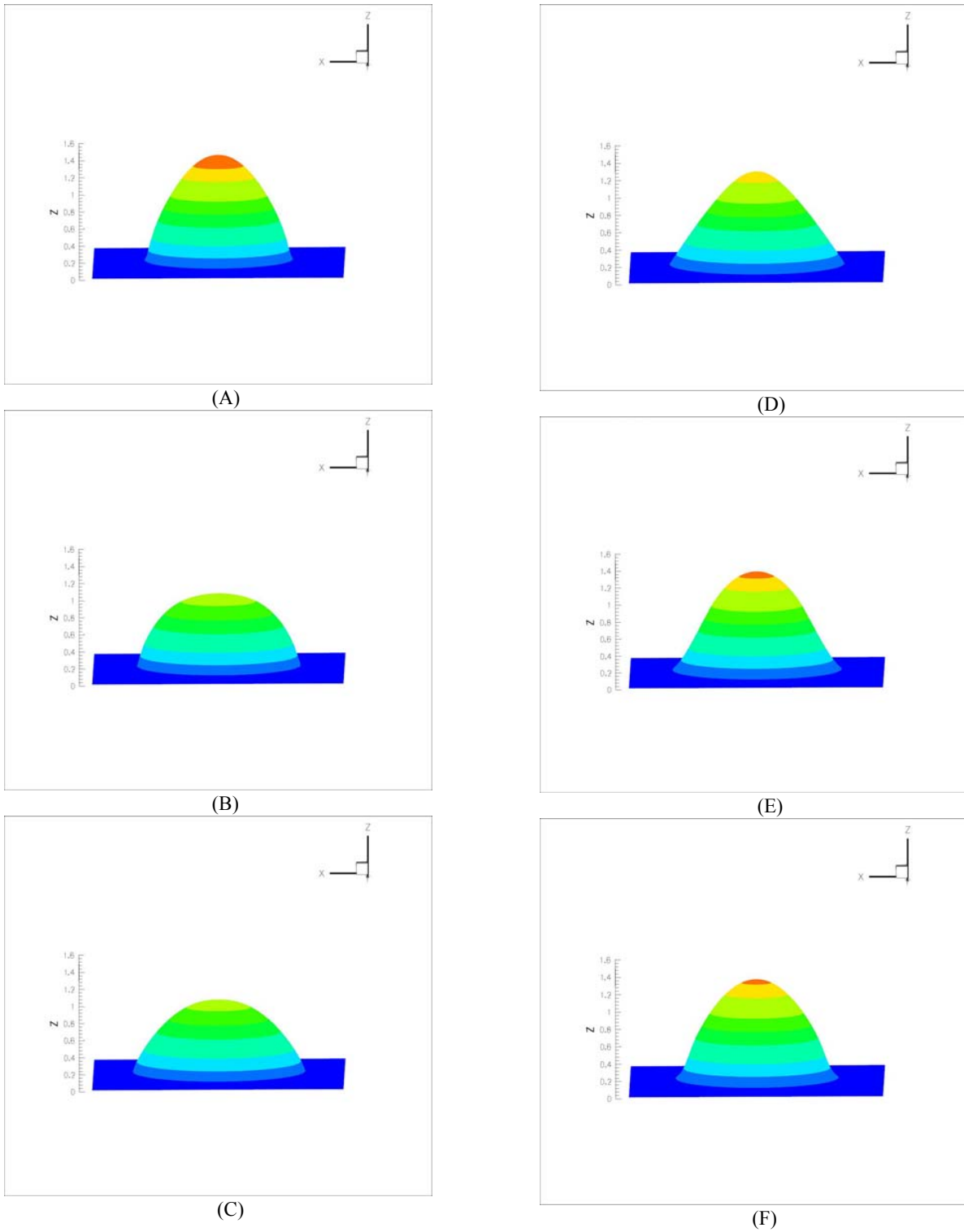


Fig. 2. Parabolic Bowl: Computed 3D water depth (h) at (A) $t = \tau/6$, (B) $t = 2\tau/6$, (C) $t = 3\tau/6$, (D) $t = 4\tau/6$, (E) $t = 5\tau/6$, (F) $t = \tau$.

order of accuracy is better than those obtained by a certain existing models; particularly for the drying stage. Also, present method efficiently conserves the total mass of the physical domain. Overall, our present method gives very satisfactory results in all aspects and it can be used as a standard method to solve this type of moving boundary problems.

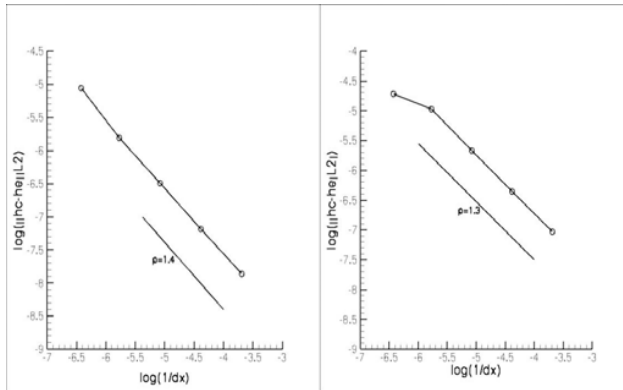


Fig. 3 Parabolic bowl: convergence rate in L^2 error norms at $t = \tau/2$ [left] and $t = \tau$ [right].

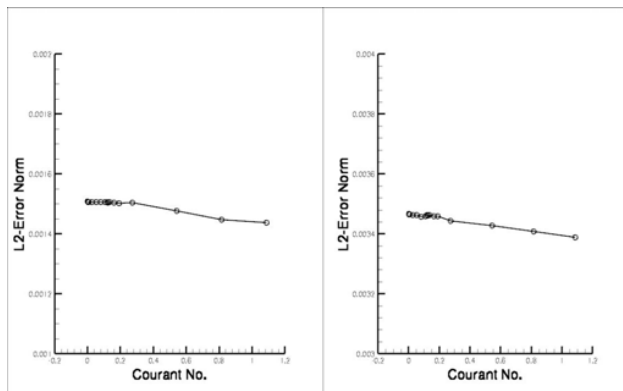


Fig. 4. Parabolic bowl: error plots for different Courant Numbers at $t = \tau/2$ [left] and at $t = \tau$ [right].

ACKNOWLEDGMENT

This work has been financially supported by the French Ministry of Ecology, Sustainable Development and Rural Management (CETMEF).

REFERENCES

- [1] S. F. Bradford and B. F. Sanders, "Finite-volume model for shallow-water flooding of arbitrary topography," *J. Hydraul. Eng., ASCE*, vol 128, no. 3, pp. 289-298, 2002.
- [2] P. Brufau, M. E. Vázquez-Cendon and P. García-Navarro, "A numerical model for the flooding and drying of irregular domains," *Int. J. Numer. Meth. Fluids*, vol 39, pp. 247-275, 2002.
- [3] S. Bunya, E. J. Kubatko, J. J. Westerink and Dawson C, "A wetting and drying treatment for the Runge–Kutta discontinuous Galerkin solution to the shallow water equations," *Comput. Methods Appl. Mech. Engrg.*, vol 198, pp. 1548–1562, 2009.
- [4] A. J. Chorin, "Numerical solution of the Navier-Stokes equations," *Math. Comput.*, vol 22, pp. 745-762, 1968.
- [5] A. Ern, S. Piperno and K. Djadel, "A well-balanced Runge–Kutta discontinuous Galerkin method for the shallow-water equations with flooding and drying," *Int. J. Numer. Meth. Fluids*, vol 58, pp. 1–25, 2008.
- [6] S. Guillou and K. D. Nguyen, "An improved technique for solving two-dimensional shallow water problems," *Int. J. Numer. Meth. Fluids*, vol 29, p. 465-483, 1999.
- [7] M. H. Kobayashi, J. M. C. Pereira and J. C. F. Pereira, J.C.F, "A conservative finite-volume second-order accurate projection method on hybrid unstructured grids," *J. Comp. Phys.*, vol 150, pp. 40-75, 1999.
- [8] K. D. Nguyen and A. Ouahsine, "2D numerical study on tidal circulation in strait of Dover," *J. of Waterway, Port, Coastal and Ocean Engineering*, vol 123, no. 1, pp. 8-15, 1997.
- [9] K. D. Nguyen, Y-E Shi, S. Wang and T. H. Nguyen, "2D Shallow-Water Model Using Unstructured Finite-Volumes Methods," *Journal of Hydraulic Engineering, ASCE*, vol 132 (3) , pp. 258-269, 2006.
- [10] C. M. Rhie and W. L. Chow, "Numerical study of the turbulent flow past an airfoil with trailing edge separation," *American Institute of Aeronautics and Astronautics (AIAA) Journal*, vol 21, no. 11, pp. 1525-1532, 1983.
- [11] J. C. Tannehill, D. A. Anderson and R. H. Pletcher Computational Fluid Mechanics and Heat Transfer. *Washington D.C.: Taylor & Francis*, 1997, ch. IV.
- [12] W. C. Thacker, "Some Exact Solutions to the Nonlinear Shallow-water Wave Equations," *J. Fluid Mech.*, vol 107, p. 499 – 508, 1981.